ISSN 1027-5495. Functional Materials, 29, No.1 (2022), p. 30-38.
doi:https://doi.org/10.15407/fm29.01.30

Detection of regularities of $Y_2Zr_2O_7$ pyrochlor phase formation during the reaction of solid-phase synthesis under different temperature-time conditions

V.O.Chyshkala[1]***, S.V.Lytovchenko***[1]***, V.P.Nerubatskyi***[2]***, R.V.Vovk***[1]***,***
E.S.Gevorkyan[2]***, O.M.Morozova***[2]

[1]V.N.Karazin Kharkiv National University, 4 Svobody Sq.,
61022 Kharkiv, Ukraine
[2]Ukrainian State University of Railway Transport, 7 Feierbakh Sq.,
61050 Kharkiv, Ukraine

Received March 22, 2021

The basic regularities of phase formation in the pyrochlor synthesis depending on temperature regimes have been investigated. The mechanisms of formation and structural-phase evolution in the synthesis of new substances and consolidation of compounds of the Y_2O_3–ZrO_2 system have been considered. Samples of an oxide sintered mass with a fraction of pyrochlorine phase $Y_2Zr_2O_7$ up to 41 % were obtained. The features of increasing the proportion of pyrochlore, which promotes the activation of a chemical reaction, either by increasing the synthesis temperature to the temperatures of eutectic formation, or by increasing the reaction surface of the powders, are considered. It is established that the kinetics of an increase in pyrochlorine phase proportion in the samples indicates the desired increase in the chemical reaction activity, which can be achieved by increasing the synthesis temperature to the temperature of eutectic formation or increasing the reaction surface of powders.

Keywords: eutectic, yttrium oxide, zirconium oxide, pyrochlor, sintering.

Виявлення закономірностей фазоутворення пірохлору $Y_2Zr_2O_7$ при проходженні реакції твердофазного синтезу за різних температурно-часових умов. *В.О.Чишкала, С.В.Литовченко, В.П.Нерубацький, Р.В.Вовк, Е.С.Геворкян, О.М.Морозова*

Досліджено основні закономірності фазоутворення при синтезі пірохлору в залежності від температурних режимів. Розглянуто механізми формування та досліджено структурно-фазову еволюцію при синтезі нових речовин та консолідації сполук системи Y_2O_3–ZrO_2. Отримано зразки оксидних спеків з часткою пірохлорної фази $Y_2Zr_2O_7$ до 41 %. Виявлено особливості збільшення частки пірохлору, яка сприяє активності хімічної реакції шляхом підвищення температури синтезу до температур утворення евтектики або збільшення реакційної поверхні порошків. Встановлено, що кінетика збільшення частки пірохлорної фази в зразках свідчить про бажане підвищення активності хімічної реакції, чого можливо досягти підвищенням температури синтезу до температур утворення евтектики або збільшенням реакційної поверхні порошків.

1. Introduction

The study of the phase formation of pyrochlor $Y_2Zr_2O_7$ during the solid-phase synthesis reaction is relevant for a number of reasons. Zirconium oxide partially stabilized with yttrium oxide is promising as an instrumental or structural material, and has great functional value [1, 2]. Another important factor is that zirconium compounds are widespread in the lithosphere; according to various data, the zirconium clarke is from 170 to 250 g/t [3]. Therefore, expanding the technological possibilities of using this material, obtaining products with a competitive market price will contribute to the promotion of zirconium products on the world market [4, 5]. The compound of zirconium oxide and yttrium pyrochloride is of great interest.

Much attention is paid to the problems to the formation of the $Y_2Zr_2O_7$ pyrochlore phase during the solid-phase synthesis reaction at different temperature and time conditions.

In [6], $Y_2Ti_2O_7$, $Y_2Zr_2O_7$, $Y_2Hf_2O_7$ were successfully synthesized using the mechanism of mechanically activated annealing (MAA) and reverse co-precipitation (RCP). The results indicate that internodal TiO_2 is soluble in the Y_2O_3 lattice. At the same time, Y_2O_3 dissolves in ZrO_2 and HfO_2 due to oxygen vacancies formed during dissolution. TG-DTA studies have given a possibility to estimate annealing and calcination temperatures. Ionic radii and melting temperatures correlate with diffusion, which is important for determining the time and temperature of phase formation for both MAC and RCP routes. RCP oxides, formed in the temperature range 700–900°C by heat treatment for 10 min. and having small $Y_2Ti_2O_7$ crystallite sizes in the range of 6–33 nm, have an ordered pyrochlor structure, which is confirmed by superlattice reflections in XRD and TEM diffraction patterns and predictions of cationic radii. $Y_2Zr_2O_7$ and $Y_2Hf_2O_7$ form defective fluorite lattices, as predicted by cationic radii. The TEM results also confirm the formation of single-phase oxides in the nanocrystalline state. Studies show that local disorder and bond length vary depending on the composition as well as on the route of synthesis. In addition, $Y_2Hf_2O_7$ has the highest local disorder and $Y_2Ti_2O_7$ has the lowest. The measurements of the Young's modulus and hardness show that $Y_2Hf_2O_7$ (obtained by the MAA route) has the highest hardness, and $Y_2Ti_2O_7$ has the highest Young's modulus, due to the order in the structure observed by XRD and Raman spectroscopy. In [7], the reactions between calcium-magnesium-aluminum silicates (CMAS) and $Gd_2Zr_2O_7$ and $2ZrO_2{\cdot}Y_2O_3$ in the temperature range of 1200–1300°C and duration of 1–100 h have been studied. The penetration depth of CMAS into the $Gd_2Zr_2O_7$ and $2ZrO_2{\cdot}Y_2O_3$ granules differs significantly depending on the interaction time. Quantitative analysis of the nature and composition of the phases observed under stationary conditions (powder/powder interaction) was performed by SEM-FEG in combination with WDS analyzes using $Gd_2Zr_2O_7$ and $2ZrO_2{\cdot}Y_2O_3$ microagglomerated nanoparticles. Faster kinetics of the gadolinium-based system is illustrated by analyzing the morphology of the reaction zone and the resulting tightness of the CMAS reaction products. The composition and amount of reaction products in the equilibrium state are very similar for the two systems, but the transition states are significantly different.

In [8], the structural changes in $Y_2Zr_2O_7$ under high pressure were studied by X-ray powder diffraction using synchrotron radiation under pressure up to 34 GPa at room temperature. A new pressure-induced phase transition from a cubic (Fm-3m) structure to a rhombic (Pnma) structure was observed at 27.3 GPa, and the phase transition was irreversible. The high-pressure orthorhombic (Pnma) phase has a larger average cation-anionic bond distance than the cubic (Fm-3m) structure, which is confirmed by an increase in the coordination number.

In [9], as possible alternatives to stabilized zirconia, the compositions of solid oxide fuel elements of pyrochlore systems $Y_2Zr_2O_7$ (YZ) and $Y_2Zr_{2-x}Mn_xO_{7-\delta}$ (YZM) (where $x = 0.025$, 0.05, 0.075, and 0.10) were studied. Such materials were prepared by the process of glycine-nitrate combustion. The obtained compounds were characterized by X-ray diffraction and thermal analysis. Round granules were obtained and annealed at different temperatures from 1000 to 1400°C. The sintering behavior of YZ and YZM was investigated to obtain information on the compaction coefficient, the relative percentage of shrinkage/expansion in the volume after heat treatment and the apparent porosity. A small level of doping Mn ($\leq$10.0 wt.%) led to an increase in conductivity values. The key features that make YZ and YZM systems attractive as fuel cell electrolytes were discussed.

In [10], yttrium zirconate ($Y_2Zr_2O_7$) single crystals with a cubic structure in the size range of 50 nm were obtained by stearic acid method (SAM) using zirconium nitrate and yttrium nitrate as raw materials, stearic acid as solvent and dispersant. The synthesis process was monitored by TG-DTA. The product was characterized by XRD, FT-IR, TEM, HRTEM, EDS and BET methods. The influence of heat treatment temperature the crystal sizes and lattice distortion of nanocrystals was studied. The $Y_2Zr_2O_7$ nanocrystals obtained by SAM were well dispersed with an average size of 20–40 nm. The interplanar distances measured from the HRTEM images were 0.294 and 0.185 nm, respectively, which coincided with the theoretical values. In addition, the photocatalytic properties of $Y_2Zr_2O_7$ nanocrystals were measured and discussed. The TEM results showed that $Y_2Zr_2O_7$ nanocrystals are polycrystals with good dispersibility. The results showed that $Y_2Zr_2O_7$ nanocrystals have a high adsorption strength due to the large surface area, and their photocatalytic activity decreases with an increase in the calcination temperature.

In [11], the stability of the $Y_2Ti_2O_7$ and $Y_2Zr_2O_7$ phases under high pressure was investigated by *ab initio* methods. Pyrochlor-structured $Y_2Ti_2O_7$ and defect-fluorite $Y_2Zr_2O_7$ react differently to high pressure. Both defect-fluorite and defect-cotunite structures of $Y_2Ti_2O_7$ are energetically more stable at high pressure, but a comparison with experimental results shows that only the transformation into a defect-fluorite structure is kinetically favorable. At high pressure, the $Y_2Zr_2O_7$ defective fluorite phase should undergo a structural transition to the defective cotunite state. Fluorite-type structures contain metals mostly in the form of large tetravalent cations. Since the Zr^{4+} ion is too small to maintain the structure of fluorite at low temperatures, a partial replacement of these ions with larger cations is necessary to prevent structural changes, although such cations usually have a lower valence. To maintain electroneutrality, it is necessary to create oxygen vacancies in the structure. Since oxides at high temperatures usually have an excess of oxygen vacancies, a further increase in their concentration with the introduction of appropriate additives slows down diffusion, prevents polymorphic transition and stabilizes the phase [12].

An important feature of the fluorite structure is the ability to maintain a high degree of substitution, which promotes ionic conductivity. Addition of CaO (or MgO) in the amount of 16 mol.% or Y_2O_3 in the amount of 8 mol.% is sufficient to form a fully stabilized zirconium oxide, the structure of which becomes a cubic solid solution without phase transformations when heated from room temperature to 2500°C. It should be noted that yttrium oxide is considered the best stabilizer of zirconium dioxide in terms of technical, technological, and economic indicators.

There are more than 30 variants of the $ZrO_2{\cdot}Y_2O_3$ phase diagram, and the obtained research results have significant differences (Fig. 1) and are very contradictory; some parts of the diagram cannot be considered reliable. Calculations performed on the analysis of approximately the same arrays of experimental data showed relatively similar results for temperatures above 1000°C, although the temperatures of a number of phase transformations differ by several tens or even hundreds of degrees, and the existence of different phases is more than 10 %.

Particle size distribution of the initial oxides, in particular, the stabilizer powder, significantly affects the phase diagram of Y_2O_3–ZrO_2. It is calculated that the addition of yttrium oxide nanoparticles changes the temperatures of phase transformations [18]. It is determined that with increasing temperature, the cubic ZrO_2 and tetragonal ZrO_2 ranges expand and the monoclinic ZrO_2 region decreases.

The difficulties of experimental studies of structural-phase transformations in the Y_2O_3–ZrO_2 system are due, firstly, to the complexity of X-ray studies at temperatures above 1800°C. Most of the results were obtained at room temperature on samples that cooled as quickly as possible from pre-melting temperatures. It is clear that it is impossible to exclude the possibility of changing the structural-phase state of the samples during cooling, even at maximum speeds [19, 20]. Secondly, at relatively low temperatures (less than 1200°C) the diffusion of cations slows down so much that it is very difficult to reach equilibrium. Thirdly, the uncertainty of the temperature limits of the martensitic transformation complicates the interpretation of the microstructure of the samples. In addition, it is necessary to take into account the influence of methods of sample preparation, particle size distribution, purity of raw materials, heat treatment and other technological factors.

At temperatures exceeding the temperatures of the monoclinic phase existence, the diagram shows a two-phase region of coexistence of monoclinic and tetragonal forms, at which there is a region of the tetragonal phase, prone to transformation. This tetragonal solid solution exists in the range of compositions from 0 to 6 mol.% yttrium oxide and on cooling transforms into a monoclinic form. At higher concentrations of yttrium oxide, there is a two-phase region

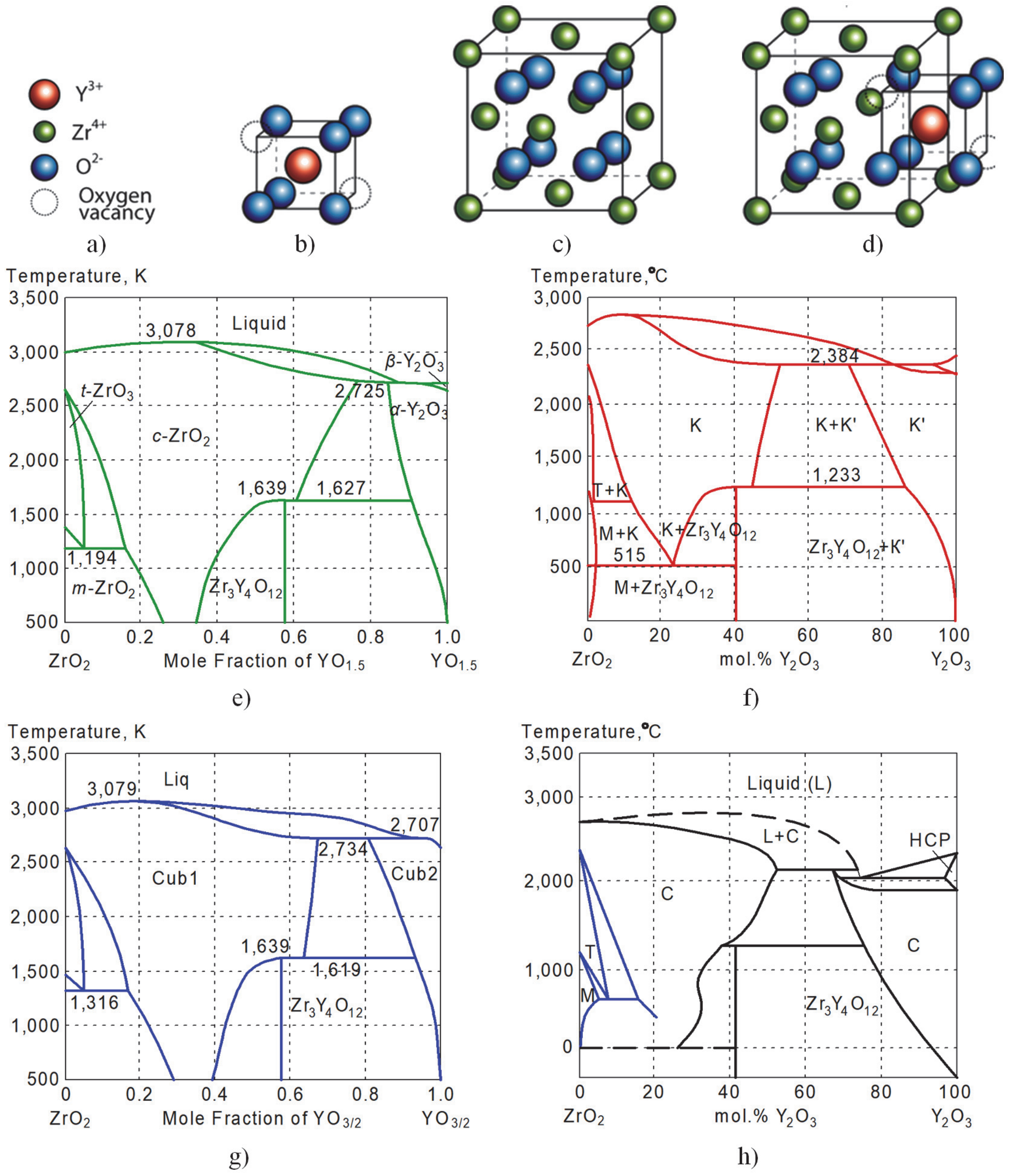

Fig. 1. Structural rearrangement during stabilization of ZrO_2 with yttrium oxide and variants of the phase diagram of $ZrO_2-Y_2O_3$ from different sources: a — elements of structures [13]; b — Y_2O_3 [13]; c — ZrO_2 [13]; d — $ZrO_2 + Y_2O_3$ (YSZ) [13]; e — [14]; f — [15]; g — [16]; h — [17].

of the tetragonal and cubic phases [21, 22]. A further increase in the concentration of yttrium oxide leads to the formation of a single-phase cubic solid solution.

The quantitative content of the stabilizer in the material has a decisive influence on the properties of ceramics [23, 24], while the excess of the stabilizer has a very negative effect on the structural stability of zirconium dioxide, due to the following reasons:

— uneven distribution of the stabilizer over the cross section of the initial powders, which is retained in the final material;

— joint release of both stabilizer-rich phase $Zr_3Y_4O_{12}$ and tetragonal phase composition ZrO_2–8.3 % Y_2O_3;

— transformation of grains of composition ZrO_2–1.6 % Y_2O_3 into a monoclinic phase;

— the influence of grain size of phase inclusions, especially fine crystalline.

Additional thermal impact on the material only enhances the segregation of the stabilizer and contributes to even greater phase heterogeneity of the material. Overcoming these complications is the task of optimizing the technological process of forming ceramic powders for further use [25, 26].

When insufficient quantity of stabilizer is added, a partially stabilized zirconium oxide, which is a mixture of cubic and metastable tetragonal ZrO_2 phases, is obtained. From the phase diagram it follows that at concentrations of stabilizing oxide less than 8 mol.%, the existence of tetragonal solid solution of zirconium dioxide is possible. The upper temperature limit of the phase stability of these solid solutions is the temperature of the phase transition t–$ZrO_2 \rightarrow c$–ZrO_2 and this temperature is lower than the melting temperature; therefore, such materials are called partially stabilized zirconia [27].

The most significant disadvantage of stabilizing zirconium dioxide by adding yttrium oxide is the tendency of this composite material to degrade in the temperature range from 25 to 400°C; this is possible in the presence of water vapor and is essentially a slow transformation of the structure into monoclinic form. The kinetics of this transformation is influenced by various technological factors (vapor pressure, gas composition, grain size, other impurities) [28, 29]. The reason for these structural changes may be the penetration of water molecules into the sites of oxygen vacancies, which significantly impairs the diffusion of ions and the overall stability of the material.

An analysis of the studies showed that the synthesized pyrochlor can be used in tribosystems with improved antifriction and anti-wear properties. In studying the properties of the composites under consideration, the main attention was paid to the mechanical characteristics of the material, especially crack resistance and hardness, tribological properties. Also, when testing on friction and wear, the influence of the structure of composites based on zirconium dioxide on wear resistance was not taken into account. Most studies have not established correlations between thermomechanical and tribological properties. There are almost no studies on the interaction and compatibility of materials of the tribosystem "ceramic composite-metal" on the friction processes in the contact zone.

Thus, the problem of revealing the patterns of phase formation of pyrochlor $Y_2Zr_2O_7$ during the reaction of solid-phase synthesis under various temperature and time conditions needs to be solved. In addition, reducing the cost of nanopowders, improving their quality, the use of modern methods of forming and sintering nanopowders creates new opportunities for the production of composite materials with high physical and mechanical properties.

The aim of the study is to reveal the patterns of phase formation of $Y_2Zr_2O_7$ pyrochlor during the reaction of solid-phase synthesis under various temperature and time conditions, which will make it possible to obtain composite materials with high physical, mechanical and operational properties. To achieve this goal, the following tasks were set:

— to study the main patterns of phase formation in the synthesis of pyrochlor depending on temperature regimes, mechanisms of formation and evolution of the structure of the materials obtained, structural and phase characteristics of the materials of various chemical compositions;

— to identify the effect of increasing the proportion of pyrochlor, which contributes to the activity of the chemical reaction;

— to evaluate the possibility of increasing the activation of the reaction surface of powders in order to achieve the formation of eutectic phases in pyrochlore.

2. Experimental

Taking into account the experience gained [30, 31] and previous attempts to use different starting compounds of yttrium [32, 33], the method of simple mixing was chosen. Sintering and synthesis of the compounds were performed at temperatures of 1200°C, 1400°C and 1500°C in air. Duration of high temperature treatment ranged from 2 to 20 hours.

Microstructure and composition of the samples were determined using electron microscopy and X-ray microanalysis. The structure of electroconsolidated samples of zirconium ceramics was studied using force probe microscopy (Ntegra Aura atomic force microscope) and raster microscopy (raster ion-electron microscope Nova NanoSEM, raster electron microscope Quanta 200 3D).

AFM-scanning was performed by the semi-contact method in air in two modes: at constant amplitude (topography) and in the phase contrast mode. Images of 1×1 μm, 2.5×2.5 μm and 5×5 μm were obtained. Chemical analysis of consolidated samples was performed using a complex of a scanning electron microscope LEO1455 VP (ZEISS, Germany) with blocks of an X-ray energy spectrometer INCA Energy-300. Phase analysis of the samples was performed

Table 1. Phase composition of individual samples formed at different temperatures and duration of exposure

No.	Temperature and duration of sintering	Phases	Weight fraction, %	Lattice parameters, Å
1	1200°C, 20 hours	Y_2O_3	48.9	10.602
	$Y_2Zr_2O_7$	18.3	10.407	
	ZrO_{2-c}	16.1	5.150	
	ZrO_{2-t}	16.7	$a = 3.607$, $c = 5.175$	
2	1400°C, 2 hours	Y_2O_3	47.8	10.596
	$Y_2Zr_2O_7$	30.6	10.424	
	ZrO_{2-c}	15.9	5.149	
	ZrO_{2-t}	5.7	$a = 3.602$m, $c = 5.173$	
3	1400°C, 5 hours	Y_2O_3	43.1	10.601
	$Y_2Zr_2O_7$	33	10.448	
	ZrO_{2-c}	16.5	5.150	
	ZrO_{2-t}	7.4	$a = 3.606$, $c = 5.173$	
4	1500°C, 2 hours	Y_2O_3	42.5	10.601
	$Y_2Zr_2O_7$	36.7	10.459	
	ZrO_{2-c}	16	5.151	
	ZrO_{2-t}	4.8	$a = 3.607$, $c = 5.182$	

using the ASTM database (American Society for Testing Materials).

X-ray phase analysis was performed using Shimadzu XRD-6000 diffractometer with the following mode: CuKα radiation ($\lambda = 1.54187$ E); a curved graphite monochromator in front of the detector; θ–2θ scanning with a step of 0.02 deg in the angular range of $2\theta = 5.0$–100.0 deg at a scanning speed of 1.2 deg/min; X-ray tube voltage is 40 kV; current is 30 mA.

The samples were polished at the Struers grinding and polishing complex (Denmark) using diamond pastes up to 1 μm.

3. Result and discussion

The phase composition of the tested samples is given in Table 1.

Analysis of Table 1 data indicates the ability to control the process of pyrochlor synthesis by changing the technological parameters of high-temperature sintering. In particular, according to X-ray data, the amount of pyrochlorine phase $Y_2Zr_2O_7$ in the obtained samples ranged from 18 % to almost 41 % (by weight), and the effect of temperature is much more significant than the duration of high temperature exposure (Fig. 2, a). Sintering temperature also affects the density of the samples, although this effect is not as significant as the effect on the pyrochlore synthesis reaction rate, which determines the content of this phase. The influence of sintering temperature-time parameters on the rate of the pyrochlore phase synthesis is shown in Fig. 2, b; Fig. 2, c shows the density of the samples.

Fig. 3, a shows the microstructure of a sample sintered at 1500°C for 5 hours, and Fig. 3, b shows the distribution of elements on the fracture surface of the sample.

Analysis of the microstructure of the sample shows that it is formed by crystallites with sizes from 100 nm to 1000 nm. Between the crystallites, there is a large number of pores of similar size. The sample also has a significant number of cracks and individual large pores up to 10 μm in size. A significant number of pores indicates the active diffusion of elements during sintering and the occurrence of reactions of the synthesis of compounds with changes in the lattice parameters and the specific lattice volume of the compounds formed. This may be the reason that significantly complicates the production of high-density ceramics under these technological conditions.

Analysis of the distribution of elements on the fracture surface (Fig. 3, b) shows

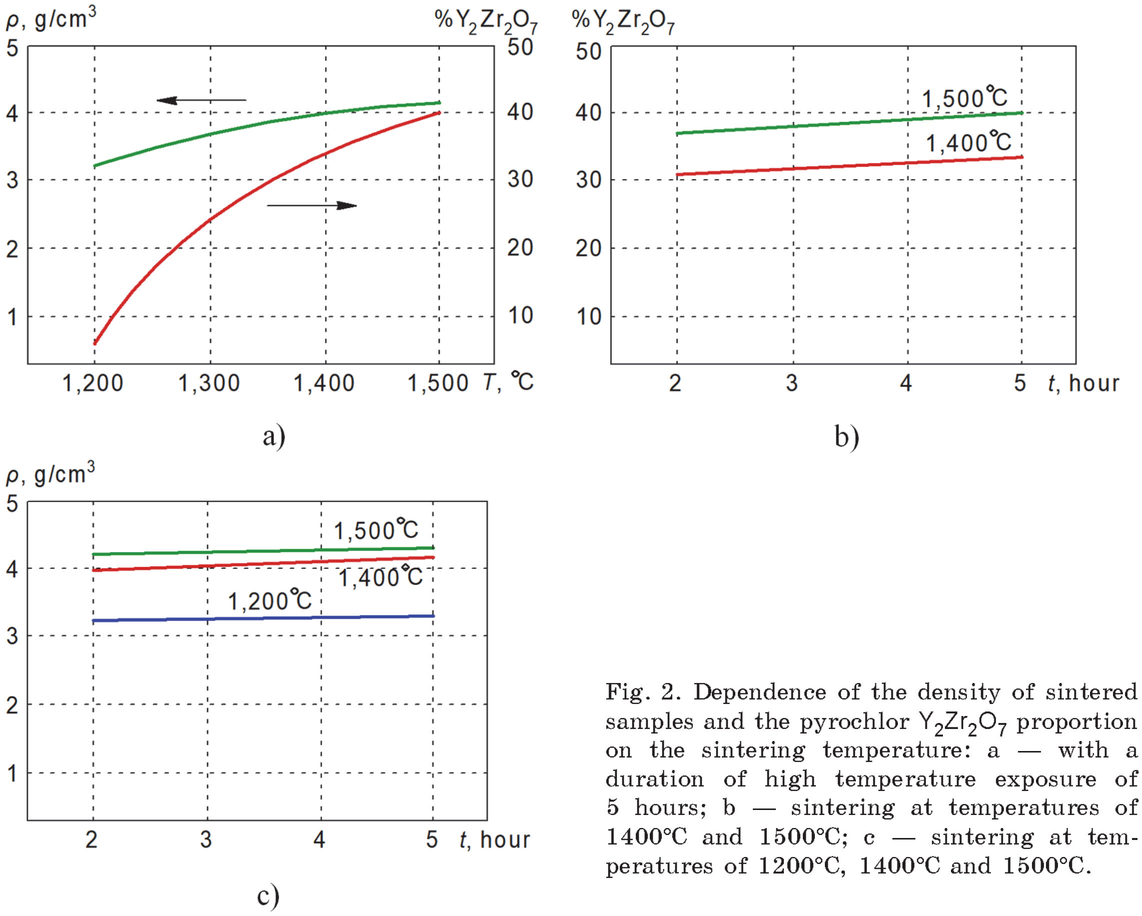

Fig. 2. Dependence of the density of sintered samples and the pyrochlor $Y_2Zr_2O_7$ proportion on the sintering temperature: a — with a duration of high temperature exposure of 5 hours; b — sintering at temperatures of 1400°C and 1500°C; c — sintering at temperatures of 1200°C, 1400°C and 1500°C.

proper uniformity over most of the surface with the exception of a few areas (Y and Zr). Samples of a mixture of yttrium and zirconium oxides pressed at a pressure of 100 MPa and sintered at 1200°C for 20 hours had an average relative density of 3.25 g/cm^3, which is about 58 % of the theoretical density of the mixture of oxides studied.

The obtained experimental data on the rate of the pyrochlor synthesis indicate the possibility of occurring this process under chosen technological conditions; however, the technology of obtaining $Y_2Zr_2O_7$ pyrochlor by burning-out a mixture of oxides at the maximum tested sintering temperature of 1500°C is not economically justified. To obtain 90 %, many hours of high-temperature exposure is required, which, according to preliminary estimates and some literature data, will be several hundred hours.

Thus, a variant of the technology was tested, according to which sintering was carried out in several stages, and after each stage of sintering, the ceramic samples were again ground and pressed, and then sintering continued. However, significant growth of the pyrochlore phase was not recorded; and the loss of material during grinding in a planetary mill was noticeable. For these reasons, this option was considered unacceptable.

To obtain samples with a higher content of pyrochlorine it is necessary:

— to increase significantly the temperature of synthesis of the oxide mixture before melting, which can be realized by electron beam method or heating in plasma;

— if the fusion synthesis is not effective, it will be necessary to involve the technology of interrupting sintering with grinding of the sintered mass;

— synthesis of pyrochlor $Y_2Zr_2O_7$ can be realized by thermal decomposition of yttrium nitrates at 800°C in an oxygen atmosphere (without nitrogen).

4. Conclusion

The basic regularities of phase formation in the synthesis of pyrochlor depending on temperature regimes were studied. The possibility of the reaction of the synthesis of the $Y_2Zr_2O_7$ phase with the pyrochlore structure from a mixture of yttrium and zirconium oxides during high-temperature sintering in air has been proved. The

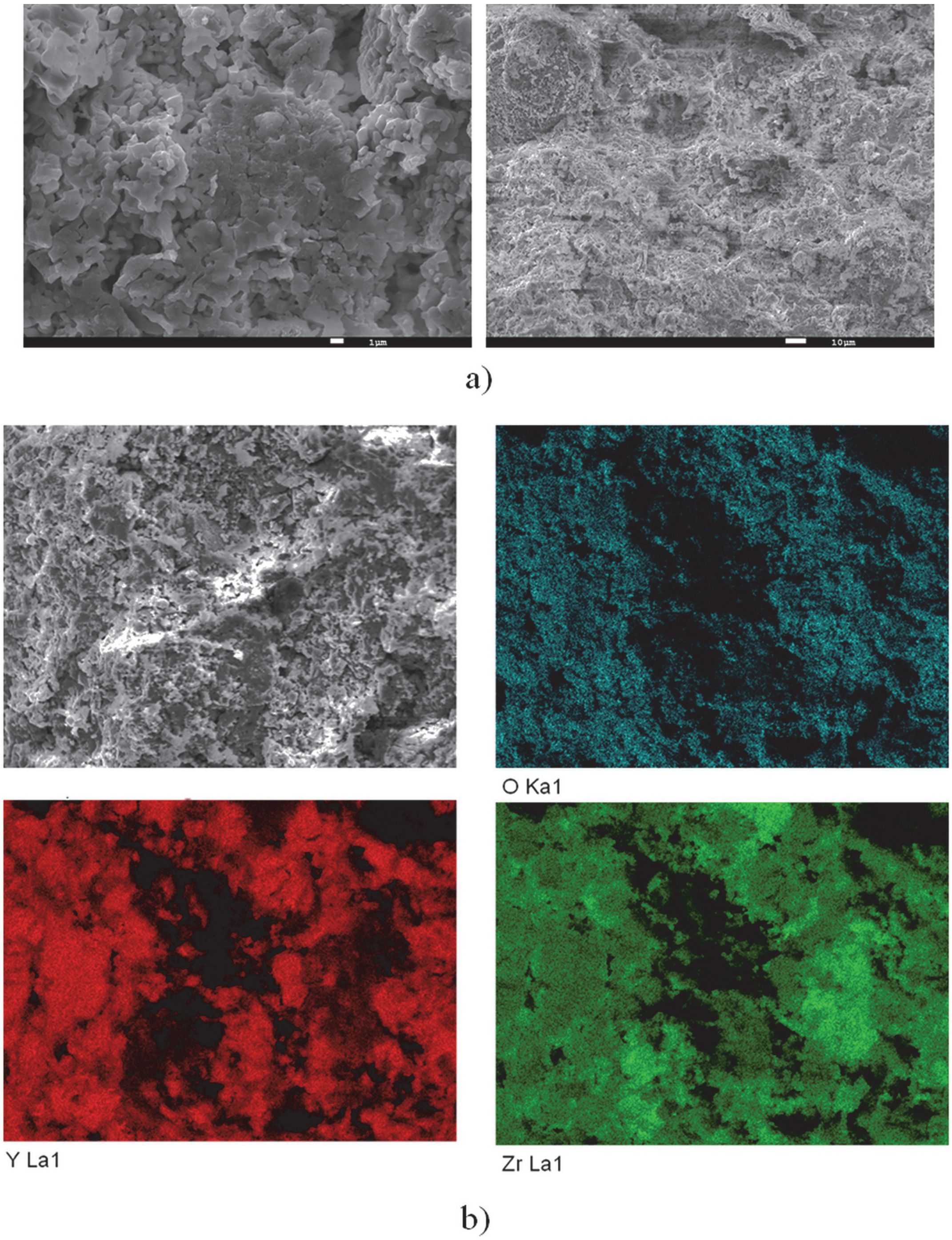

Fig. 3. Microstructure of a Y_2O_3–$2ZrO_2$ sample, sintered at 1500°C for 5 hours (JSM — 700IF) (a), distribution of elements on the fracture surface of the sample (b).

mechanisms of formation and structural-phase evolution during the synthesis of new substances and consolidation of compounds of the Y_2O_3–ZrO_2 system were considered. The reaction rate of the synthesis of the $Y_2Zr_2O_7$ phase depends on the temperature and time parameters of sintering, with the influence of temperature being the determining one. Samples of oxide sintered mass with a fraction of pyrochlorine phase $Y_2Zr_2O_7$ up to 41 % were obtained.

The peculiarities of increasing the proportion of pyrochlor, which promotes the activity of the chemical reaction by increasing the temperature of synthesis to the temperatures of eutectic formation or increasing the reaction powders surface, are considered. The applied temperatures (up to

1500°C) are insufficient for the necessary intensification of the $Y_2Zr_2O_7$ phase synthesis and its completion. The kinetics of increasing the pyrochlorine phase proportion in the samples indicates the desired increase in the chemical reaction activity, which can be achieved by increasing the synthesis temperature to the temperatures of eutectic formation or increasing the powders surface reaction.

References

1. V.O.Chyshkala, S.V.Lytovchenko, E.S.Gevorkyan et al., *SWorldJournal*, **7**, 17 (2021).
2. O.Morozova, V.Nerubatskyi, in: International Scientific Interdisciplinary Conference ISIC-2021 for Medical Students and Young Scientist, Kharkiv, Ukraine (2021), p.25.
3. E.Gevorkyan, V.Nerubatskyi, V.Chyshkala et al., *Eastern-European Journal of Enterprise Technologies*, **5**, 6 (2021).
4. Q.Li, X.Hao, Y.Gui et al., *Ceramics International*, **47**, 27188 (2021).
5. M.Boniecki, T.Sadowski, P.Golebiewski et al., *Ceramics International*, **46**, 1 (2019).
6. G.Karthick, A.Karati, B.S.Murty, *Journal of Alloys and Compounds*, **837**, 155491 (2020).
7. S.Duluard, E.Delon, J.-P.Bonino et al., *Journal of the European Ceramic Society*, **39**, 1451 (2018).
8. H.Li, Q.Tao, N.Li et al., *Journal of Alloys and Compounds*, **660**, 446 (2016).
9. M.Kumar, I.Arul Raj, R.Pattabiraman, *Materials Chemistry and Physics*, **108**, 102 (2008).
10. Y.Tong, P.Xue, F.Jian et al., *Materials Science and Engineering: B*, **150**, 194 (2008).
11. H.Y.Xiao, F.Gao, W.J.Weber, *Physical Review B*, **80**, 212102 (2009).
12. A.V.Belyakov, *Glass and Ceramics*, **3**, 19 (1999).
13. S.Sikarwar, B.C.Yadav, S.Singh et al., *Sensors and Actuators B: Chemical*, **232**, 283 (2016).
14. M.Chen, B.Hallstedt, L.Gauckler, *Solid State Ionics*, **170**, 255 (2014).
15. S.A.Degtyarev, G.F.Voronin, *Journal Physical Chemistry*, **LXI**, 611 (1987).
16. O.Fabrichnaya, F.Aldinger, *Zeitschrift fur Metallkunde*, **95**, 27 (2004).
17. L.Wang, X.H.Zhong, Y.X.Zhao et al., *Journal of Asian Ceramic Societies*, **2**, 102 (2014).
18. M.Asadikiya, H.Sabarou, M.Chen et al., *RSC Advances*, **6**, 17438 (2016).
19. E.Gevorkyan, M.Rucki, T.Salacinski et al., *Materials*, **14**, 12 (2021).
20. E.Gevorkyan, M.Rucki, Z.Krzysiak et al., *Materials*, **14**, 6503 (2021).
21. Yu.M.Polezhaev, *ZhFKh*, **41**, 2958 (1967).
22. A.V.Belyakov, *Glass and Ceramics*, **2**, 16 (1999).
23. E.S.Gevorkyan, M.Rucki, A.A.Kagramanyan et al., *International Journal of Refractory Metals and Hard Materials*, **82**, 336 (2019).
24. V.M.Arzhavitin et al., *VANT*, **5**, 58 (2013).
25. E.Gevorkyan, V.Nerubatskyi, Yu.Gutsalenko et al., *Eastern-European Journal of Enterprise Technologies*, **6**, 41 (2020).
26. E.S.Gevorkyan, V.P.Nerubatskyi, Yu.H.Gutsalenko et al., *Modern Engineering and Innovative Technologies*, **14**, 46 (2020).
27. C.B.Starostenko, V.M.Voevodin, M.A.Tikhonovsky et al., *Physico-chemical Mechanics of Materials*, **51**, 70 (2015).
28. .V.Alisin, M.A.Borik, A.V.Kulebyakin et al., *Inorganic Materials*, **6**, 609 (2015).
29. V.V.Okovityi, *Science and Technology*, **5**, 26 (2015).
30. E.S.Gevorkyan, V.P.Nerubatskyi, V.O.Chyshkala et al., *Modern Engineering and Innovative Technologies*, **15**, 6 (2021).
31. E.Gevorkyan, A.Mamalis, R.Vovk et al., *Journal of Instrumentation*, **16**, P10015 (2021).
32. V.A.Skuratov, A.S.Sohatsky, J.H.O'Connell et al., *J.Nucl.Mater.*, **456**, 111 (2015).
33. P.Melnikov, V.A.Nascimento, L.Z.Consolo et al., *J.of Therm.Analysis and Calorimetry*, **111**, 115 (2013).